

# A study of the vacuum pyrolysis of para-substituted diazoacetophenones with He(I) ultraviolet photoelectron spectroscopy

Nick H. Werstiuk, Heidi M. Muchall, Jiagong Ma, and Michael T.H. Liu

**Abstract:** An ultraviolet photoelectron (PE) spectrometer apparatus that utilizes a tuneable 50 W CW CO<sub>2</sub> laser as a directed heat source was used to study the vacuum pyrolysis of diazoacetophenone (**1a**) and its *p*-methyl, *p*-methoxy, *p*-chloro, and *p*-nitro analogues **1b**, **1c**, **1d**, and **1e**. Analysis of the pyrolysate with He(I) ultraviolet PE spectroscopy shows that at a laser power level of 26 W (500 ± 50°C) **1a**, **1b**, **1c**, and **1d**, cleanly yield the corresponding phenylketenes **2a**, **2b**, **2c**, and **2d**, respectively, the products of the Wolff rearrangement of the incipient ketocarbenes. Of this group of highly reactive ketenes, which cannot be isolated in the condensed phase at ambient temperature, only **2a** has been the subject of a previous PE spectroscopic study. But our work indicates that the sample of **2a** prepared in the earlier study was impure. The low volatility of *p*-nitrodiazoacetophenone (**1e**) thwarted our attempts to generate **2e** and obtain its spectrum. Calculations at semiempirical (AM1) and ab initio (HF/6-31G(d)) levels of theory established that the diazoacetophenones prefer to adopt twisted *syn* conformations. That the calculated ionization potentials (HAM/3 and Becke3LYP/6-31+G(d)//HF/6-31G(d)) of **1a–1d** and the synthesized PE spectra of **1a**, **1b**, and **1c** correlate well with the PE spectroscopic data supports this finding. Shifts observed in the three low-energy ionizations of ketenes **2b**, **2c**, and **2d** induced by the *para*-substitution can be related to the character of the corresponding occupied molecular orbitals of phenylketene (**2a**).

*Key words:* diazoacetophenones, phenylketenes, He(I) photoelectron spectroscopy, thermolysis, quantum chemical calculations.

**Résumé :** On a fait appel à un spectromètre photoélectronique (PE) ultraviolet, qui utilise comme source de chaleur un laser à CO<sub>2</sub> de 50 W ajustable et à VC, pour étudier la pyrolyse sous vide de la diazoacétophénone (**1a**) et de ses analogues *p*-méthyl-, *p*-méthoxy-, *p*-chloro- et *p*-nitro- (**1b**, **1c**, **1d** et **1e**). L'analyse des pyrolysats par spectroscopie PE ultraviolette à He(I) montre que, à une puissance de laser de 26 W (500 ± 50°C), les composés **1a**, **1b**, **1c** et **1d** conduisent proprement aux phénylcétènes correspondants, soit les produits **2a**, **2b**, **2c** et **2d** respectivement, qui correspondent aux produits de réarrangement de Wolff des céto-carbènes qui se forment. De ce groupe de cétones hautement réactifs qui ne peuvent pas être isolés sous forme condensée à la température ambiante, seul le composé **2a** avait fait l'objet d'une étude antérieure par spectroscopie PE. Les résultats obtenus au cours de ce travail indiquent toutefois que le composé **2a** préparé antérieurement n'était pas pur. La faible volatilité de la *p*-nitrodiazoacétophénone (**1e**) nous a empêché de générer le produit **2e** et d'en obtenir un spectre. Des calculs théoriques aux niveaux semiempirique (AM1) et ab initio (HF/6-31G(d)) ont permis de déterminer que les diazoacétophénonnes adoptent préférentiellement les conformations *syn* déformées. Le fait que les potentiels d'ionisation calculés (HAM/3 et Becke3LYP/6-31+G(d)//HF/6-31G(d)) pour les composés **1a–1d** et que les spectres PE synthétisés des produits **1a**, **1b** et **1c** donnent une excellente corrélation avec les données de spectroscopie PE est en accord avec cette conclusion. Les déplacements observés dans les trois ionisations de faible énergie des cétones **2b**, **2c** et **2d** sont induits par les substituants en *para* et on peut les relier au caractère des orbitales moléculaires occupées correspondantes du phénylcétène (**2a**).

*Mots clés :* diazoacétophénonnes, phénylcétènes, spectroscopie photoélectronique He(I), thermolyse, calculs théoriques par chimie quantique.

[Traduit par la Rédaction]

Received March 26, 1998.

**N.H. Werstiuk**,<sup>1</sup> **H.M. Muchall**,<sup>1</sup> and **J. Ma**. Department of Chemistry, McMaster University, Hamilton, ON L8S 4M1, Canada. **M.T.H. Liu**. Department of Chemistry, University of Prince Edward Island, Charlottetown, PE C1A 4P3, Canada.

<sup>1</sup>Authors to whom correspondence may be addressed. Telephone: (905) 525-9140. Fax: (905) 522-2509. E-mail: werstiuk@mcmaster.ca; muchall@mcmaster.ca

**Fig. 1.** Optimized structures of (a) **1a–1e** obtained with AM1 and (b) **1a–1d** obtained with HF/6-31G(d).

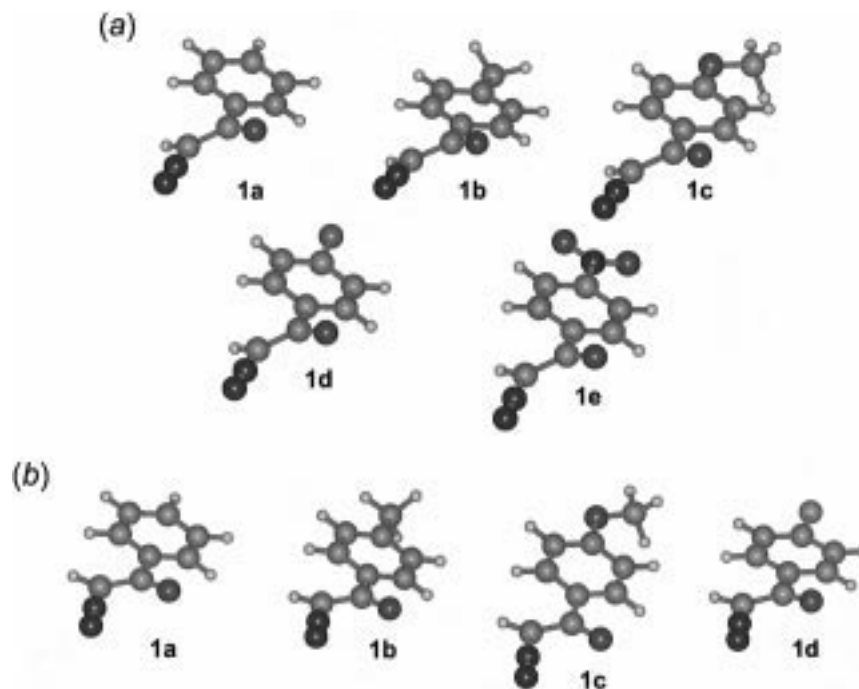
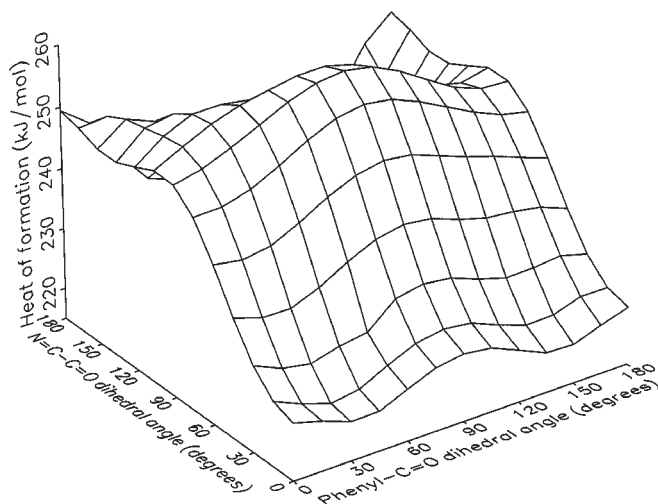


**Fig. 2.** Potential energy surface (AM1) of **1a** for the torsion of N=C—C=O and phenyl—C=O dihedral angles.



## Introduction

To facilitate the preparation and detection of highly reactive transients in the gas phase, we developed a He(I) ultraviolet photoelectron (PE) spectrometer-CW CO<sub>2</sub> laser apparatus and used it successfully to study the vacuum pyrolysis of 6,6-dihalobicyclo[3.1.0]hexanes (1), 1,2,3-benzotriazines (2), 4-diazoisochroman-3-one (3), and 4-diazoisothiochroman-3-one (4), 11-oxatricyclo[6.2.1.0<sup>2,7</sup>]-undeca-2,9-diene (5), and 2,2-dimethoxy-5,5-dimethyl- $\Delta^3$ -1,3,4-oxadiazoline (6). To widen our research in this field, we undertook a study of the vacuum pyrolysis of diazoacetophenone (**1a**), *p*-

methyldiazoacetophenone (**1b**), *p*-methoxydiazoacetophenone (**1c**), *p*-chlorodiazoacetophenone (**1d**), and *p*-nitrodiazoacetophenone (**1e**) that are potential precursors of ketocarbenes and the corresponding *para*-substituted phenylketenes, which are the Wolff rearrangement products (7). Only a limited number of ketenes which cannot be isolated in the condensed phase at ambient temperature have been studied in the gas phase with PE spectroscopy (5, 8–13), and there is comparatively little experimental data available on the vacuum pyrolysis of  $\alpha$ -diazocarbonyl compounds (see, for example, ref.14) in contrast to the large body of work that has been accumulated on the photochemistry of this class of compounds (14–21). Given that a wide variety of diazocarbonyl compounds can be synthesized (14) and, as our studies have shown, easily pyrolyzed in the gas phase, we expected PE spectroscopic and calculational studies to provide fundamental information on aspects of the electronic structure and reactivity of this group of compounds and the products derived from the incipient ketocarbenes (4, 5). We undertook a study of **1a**, **1b**, **1c**, **1d**, and **1e** specifically (i) to gain information about the nature of the frontier molecular orbitals (MOs), (ii) to study the conformational properties of these compounds in the gas phase, (iii) to establish whether our instrument is generally useful for preparing and studying ketenes in the gas phase (five new *para*-substituted phenylketenes were to be prepared), and (iv) to determine the effect of the *para*-substituents on the ionization potentials of **2a** with the goal of characterizing its highest occupied molecular orbitals. This paper documents the results of a PE spectroscopic study of the pyrolysis of diazoacetophenones **1a**, **1b**, **1c**, and **1d** and a computational study of the conformational properties and molecular orbitals of this group of compounds, the nitro analogue **1e**, and the corresponding ketenes (Scheme 1).

**Table 1.** The AM1 heats of formation  $\Delta H_f$  (kJ mol<sup>-1</sup>) and HF/6-31G(d) total energies  $E_T$  of two conformations of diazoacetophenones **1a–1e** and of phenylketenes **2a–2d**.

Compound	$\Delta H_f$	$\Delta\Delta H_f$	$E_T$ (hartrees)	$\Delta E_T$ (kJ mol <sup>-1</sup> )
<i>syn-1a</i>	221.42		-490.141 659 <sup>a</sup>	
<i>anti-1a</i>	232.55	11.13	-490.135 222 <sup>a</sup>	16.88
<i>syn-1b</i>	188.87		-529.179 538	
<i>anti-1b</i>	199.95	11.08	-529.173 039	17.05
<i>syn-1c</i>	60.54 <sup>b</sup>		-604.023 915	
<i>anti-1c</i>	72.68	12.13	-604.017 046	18.02
<i>syn-1d</i>	192.67		-949.041 019	
<i>anti-1d</i>	205.06	12.38		
<i>syn-1e</i>	240.75			
<i>anti-1e</i>	253.05	12.30		
<b>2a</b>	72.22		-381.274 201	
<b>2b</b>	40.25		-420.311 107	
<b>2c</b>	-85.40 <sup>b</sup>		-495.153 149	
<b>2d</b>	42.55		-840.173 832	

<sup>a</sup> The total energies obtained with the keyword TIGHT are identical within 10<sup>-6</sup> hartrees to the values given.

<sup>b</sup> The stereoisomer with the methoxy group orientated *anti* to the C=O group is marginally higher in energy (**1c**:  $\Delta H_f = 61.17$  kJ mol<sup>-1</sup>; **2c**:  $\Delta H_f = -85.23$  kJ mol<sup>-1</sup>) than the corresponding *syn* isomer.

**Table 2.** Selected calculated<sup>a</sup> dihedral angles (degrees) of two conformations of diazoacetophenones **1a–1e**.

Compound	Dihedral	
	N=C—C=O	phenyl—C=O
<i>syn-1a</i>	4.1(2.2) <sup>b</sup> (1.6) <sup>c</sup>	31.6(17.0) <sup>b</sup> (17.3) <sup>c</sup>
<i>anti-1a</i>	179.9(165.2) <sup>b</sup> (165.2) <sup>c</sup>	58.6(36.8) <sup>b</sup> (36.7) <sup>c</sup>
<i>syn-1b</i>	4.1(2.1) <sup>b</sup>	30.0(15.0) <sup>b</sup>
<i>anti-1b</i>	173.4(164.6) <sup>b</sup>	53.9(35.1) <sup>b</sup>
<i>syn-1c</i>	4.3(1.7) <sup>b</sup>	31.3(10.3) <sup>b</sup>
<i>anti-1c</i>	172.1(163.3) <sup>b</sup>	52.3(32.2) <sup>b</sup>
<i>syn-1d</i>	2.9	35.9
<i>anti-1d</i>	178.9	81.2
<i>syn-1e</i>	2.4	38.1
<i>anti-1e</i>	175.7	60.3

<sup>a</sup> Unless stated otherwise the values listed were calculated with AM1.

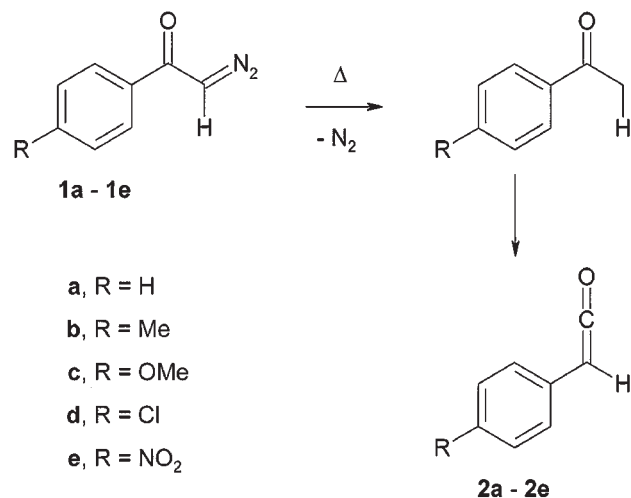
<sup>b</sup> Calculated at the HF/6-31G(d) level of theory.

<sup>c</sup> Calculated at the HF/6-31G(d) level of theory with the keyword TIGHT.

## Experimental

### Calculations

Calculations at the semiempirical level of theory were carried out with AM1 of HyperChem 4.0 (22), AMPAC 2.0 (23), or MOPAC 6.0 (24), with the latter two programs running on IBM RS/6000 model 320H, 350, and 530 computers. An RMS gradient of 0.02 was used to obtain optimized geometries with HyperChem 4.0, and the keyword PRECISE was used in the case of AMPAC and MOPAC calculations to tighten the convergence criteria. Ab initio HF (25) and Becke3LYP (26) calculations were carried out with GAUSSIAN 94 (27) running on IBM RS/6000 model 350, 530, 39H, and SP2 and SGI R10000 Impact computers. Optimized geometries were shown to be minima by frequency calculations; total energies are uncorrected for zero-point energies. The semiempirical method HAM/3 (28) was used to compute the ionization potentials. The acronyms

**Scheme 1.**

HAM/3//AM1 and HAM/3//HF/6-31G(d) indicate that HAM/3 calculations were carried out on AM1 and HF/6-31G(d) optimized equilibrium geometries, respectively. Synthetic spectra were calculated from the MO results with a FORTRAN program PESPEC (29). Spectra were synthesized from the 10 lowest IPs (HAM/3), with a Gaussian convolution of 0.4 and the temperature set at 300 K. Graphical representations of the computationally determined eigenvectors (AM1/HF/6-31G(d)) were plotted from HyperChem 4.0.

### PE spectroscopic studies

The locally built PE spectrometer-CW CO<sub>2</sub> infrared laser apparatus (the laser is used as a directed heat source) employed in this study is described in our earlier publications (1–5). To obtain the PE spectra of the diazoacetophenones (**1a**, mp 51–52; **1b**, mp 57–58; **1c**, mp 87–88; **1d**, mp 115–116; **1e**, mp 116–117°C), which were prepared by established methods (30), a 20 mg sample was placed in a bottle-shaped quartz reaction vessel that was inserted into the tip of a heated probe. The temperature was slowly ramped up (a

**Table 3.** Calculated vertical ionization potentials IP (eV) and orbital energies  $\epsilon$  (eV) for diazoacetophenones<sup>a</sup> **1a–1d** and phenylketenes **2a–2d**.

<b>1a</b>	HAM3 <sup>b</sup>	IP	8.60	9.09	9.53	9.60	11.74	11.96	12.33	12.72	13.22	13.83
	HAM3 <sup>c</sup>	IP	8.72	9.47	9.58	9.66	11.87	12.15	12.49	13.10	13.68	13.88
	B3LYP <sup>d</sup>	– $\epsilon$	6.87	7.21	7.41	7.47	9.82	10.17	10.24	11.37	11.61	12.01
		IP <sup>e</sup>	8.8	9.1	9.3	9.4	11.7	12.1	12.1	13.3	13.5	13.9
<b>1b</b>	HAM3 <sup>b</sup>	IP	8.41	9.07	9.24	9.39	11.39	11.86	12.14	12.46	12.71	12.90
	HAM3 <sup>c</sup>	IP	8.55	9.28	9.36	9.38	11.51	11.98	12.19	12.82	12.95	13.34
	B3LYP <sup>d</sup>	– $\epsilon$	6.77	7.05	7.27	7.34	9.62	9.89	9.96	10.85	11.49	11.88
		IP <sup>e</sup>	8.6	8.9	9.1	9.1	11.4	11.7	11.8	12.7	13.3	13.7
<b>1c</b>	HAM3 <sup>b</sup>	IP	8.28	8.75	8.95	9.43	10.84	11.27	12.05	12.24	12.43	12.64
	HAM3 <sup>c</sup>	IP	8.35	8.77	9.28	9.42	10.95	11.46	12.33	12.45	12.83	12.91
	B3LYP <sup>d</sup>	– $\epsilon$	6.46	6.80	7.16	7.43	9.13	9.32	10.24	10.63	10.87	11.32
		IP <sup>e</sup>	8.2	8.5	8.9	9.1	10.8	11.0	11.9	12.3	12.6	13.0
<b>1d</b>	B3LYP <sup>d</sup>	– $\epsilon$	7.00	7.25	7.51	7.77	8.93	9.46	10.32	10.76	11.04	11.69
		IP <sup>e</sup>	8.8	9.1	9.3	9.6	10.7	11.3	12.1	12.6	12.8	13.5
<b>2a</b>	HAM3 <sup>b</sup>	IP	8.17	9.36	10.19	11.99	12.03	12.27	13.35	13.80	14.04	14.21
	B3LYP <sup>d</sup>	– $\epsilon$	5.97	7.15	8.20	9.62	9.86	10.47	11.45	11.74	12.14	12.55
		IP <sup>e</sup>	7.9	9.1	10.1	11.5	11.8	12.4	13.4	13.6	14.0	14.5
<b>2b</b>	HAM3 <sup>b</sup>	IP	7.93	9.20	9.83	11.73	11.84	12.10	12.56	13.01	13.54	13.74
	B3LYP <sup>d</sup>	– $\epsilon$	5.79	7.07	7.93	9.43	9.66	10.18	10.63	11.23	11.61	11.65
		IP <sup>e</sup>	7.7	9.0	9.8	11.3	11.6	12.1	12.5	13.1	13.5	13.6
<b>2c</b>	HAM3 <sup>b</sup>	IP	7.67	9.17	9.33	11.13	11.25	12.15	12.21	12.60	13.25	13.35
	B3LYP <sup>d</sup>	– $\epsilon$	5.52	7.15	7.46	9.11	9.35	10.03	10.48	10.68	11.48	11.81
		IP <sup>e</sup>	7.4	9.1	9.4	11.0	11.3	11.9	12.4	12.6	13.4	13.7
<b>2d</b>	B3LYP <sup>d</sup>	– $\epsilon$	6.08	7.53	7.97	8.70	9.68	10.18	10.47	11.18	11.75	12.15
		IP <sup>e</sup>	7.9	9.3	9.8	10.5	11.5	12.0	12.3	13.0	13.6	14.0

<sup>a</sup>Twisted *syn* conformers.<sup>b</sup>At the HAM/3//AM1 level of theory.<sup>c</sup>At the HAM/3//HF/6-31G(d) level of theory.<sup>d</sup>At the Becke3LYP/6-31+G(d)//HF/6-31G(d) level of theory.<sup>e</sup>Orbital energies shifted uniformly, so that the HOMO energy<sup>d</sup> equals the calculated first IP<sub>v</sub> as given in Table 4.

maximum temperature of 80°C was used) until a suitable source pressure in the region of ( $3 \times 10^{-3}$ )–( $8 \times 10^{-3}$ ) Torr (1 Torr = 133.3 Pa) was obtained. In the case of **1b**, **1c**, and **1d**, which exhibited low volatilities, N<sub>2</sub> was used as a pressure make-up gas to improve the signal to noise.<sup>2</sup> Consequently, vertical expansions of the spectra were required in the region of 8–15 eV.

Spectra were obtained by averaging 20–35 scans and calibrated with the 15.6 eV band of N<sub>2</sub>. Linearity of the scale was ensured through calibrations with methyl iodide (9.54 and 10.16 eV) and O<sub>2</sub> (12.30 eV) performed prior to the experiments. Vertical ionization potentials are accurate to  $\pm 0.05$  eV. Pyrolyses of the diazoacetophenones were carried out in a hot zone 1–2 mm in length obtained by focusing the laser beam (power levels of 26, 42, and 47 W were used) on the tip (2–3 mm inner diameter) of the bottle-shaped quartz sample vessel. Due to the very low volatility of **1e** we were not able to obtain its spectrum and study its pyrolysis even in the presence of the pressure make-up gas. Hatched bands in the PE spectra are due to traces of H<sub>2</sub>O (12.6 eV) and a shadow peak (13.6 eV) of N<sub>2</sub>.

## Results and discussion

### Calculations

#### 1. Conformational properties of diazoacetophenones and phenylketenes

Figure 1(a) shows the AM1 optimized geometrical structures of the *syn* forms of **1a–1e**. The gas-phase torsional potential energy surfaces of **1a**, **1b**, and **1c** were calculated with AM1 by varying the N=C–C=O and phenyl–C=O dihedral angles from 0° to 180° in 15° increments. At the AM1 level, **1a** prefers a twisted *syn* rather than an *anti* conformation of the N=C–C=O group, and the conformer with the N=C–C=O and phenyl–C=O dihedral angles fixed at 90° is the highest energy species. Because the potential energy surfaces of **1a–1c** exhibit very similar topologies we report only the surface obtained for diazoacetophenone (**1a**) as Fig. 2. That the surfaces of **1b** and **1c** (not shown) are virtually identical to the surface of **1a** indicates that **1a**, **1b**, and **1c** have similar conformational properties in the gas phase. That twisted *syn* conformers are

<sup>2</sup>Although He(I) PE spectra of **1a**, **1b**, and **1d** already have been reported by Modelli et al. (31) they are presented again for two reasons: (i) the spectra reported earlier contain bands of nitrogen — and along with these, bands of further products — due to decomposition of the compounds, and (ii) the different analyzer transmission functions of the spectrometers used in the previous and in this study lead to PE spectra that differ in intensities of the bands. As we planned to record pyrolyses spectra, knowledge of the actual appearance of the spectra of the starting compounds taken with our instrument was essential.

**Table 4.** Total energies (hartrees) of diazoacetophenones<sup>a</sup> **1a–1d** and phenylketenes **2a–2d** (N electrons) and their radical cations<sup>b</sup> (N – 1 electrons) as well as derived first vertical ionization potentials IP<sub>v</sub> (eV).

	Number of electrons	B3LYP/6-31+G(d)//HF/6-31G(d)	
		Total energy	IP <sub>v</sub>
<b>1a</b>	N	-493.149 931	8.81
	N-1	-492.826 329	
<b>1b</b>	N	-532.468 968	8.56
	N-1	-532.154 406	
<b>1c</b>	N	-607.677 699	8.17
	N-1	-607.377 936	
<b>1d</b>	N	-952.745 171	8.75
	N-1	-952.423 728	
<b>2a</b>	N	-383.668 080	7.93
	N-1	-383.376 646	
<b>2b</b>	N	-422.986 065	7.68
	N-1	-422.703 768	
<b>2c</b>	N	-498.192 693	7.36
	N-1	-497.922 314	
<b>2d</b>	N	-843.263 383	7.94
	N-1	-842.971 686	

<sup>a</sup> Twisted *syn* conformers.

<sup>b</sup> Single-point energy calculations on the optimized molecule (N electrons) geometries.

**Table 5.** Selected experimental vertical ionization potentials IP (eV) of diazoacetophenones **1a–1d** and phenylketenes **2a–2d**.

Compound	IP			
<b>1a</b>	9.10		9.6 <sup>a</sup>	11.86
<b>1b</b>	8.78	9.00	9.19	9.41
<b>1c</b>	8.71	9.12	9.6 <sup>b</sup>	11.01
<b>1d</b>	9.14	9.33	9.59	9.78
<b>2a</b>	8.23	9.34	10.41	11.78
<b>2b</b>	8.22	9.36	10.17	11.38
<b>2c</b>	7.91	9.22	9.56	11.09
<b>2d</b>	8.29	9.25	9.74	10.55

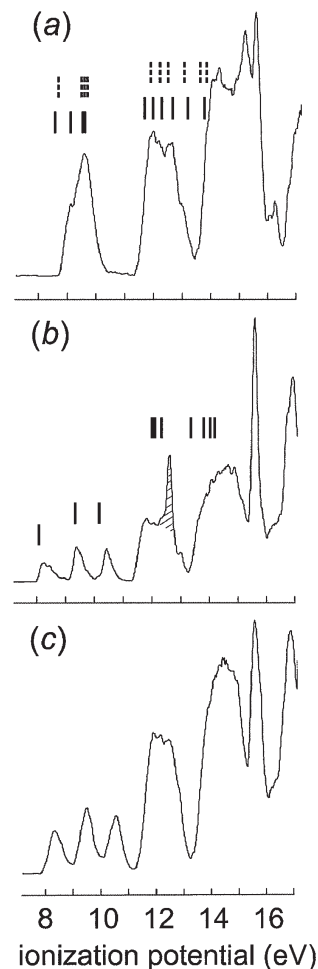
<sup>a</sup> Consists of three overlapping bands.

<sup>b</sup> Consists of two overlapping bands.

the low-energy structures in the cases of **1d** and **1e** as well indicates that the diazoacetophenones which are the subject of this study prefer to adopt twisted *syn* conformations in the gas phase.

At the AM1 level, the twisted *syn* isomers of **1a–1e** (the N=C—C=O twist angles are 4.1, 4.1, 4.3, 2.9, and 2.4°; the phenyl—C=O dihedral angles are 31.6, 30.0, 31.3, 35.9, and 38.1°, respectively) are 11.08–12.38 kJ mol<sup>-1</sup> lower in energy than the twisted *anti* isomers (Table 1). The *syn* and *anti* isomers of **1a**, **1b**, and **1c** were also studied at the HF/6-31G(d) level of theory. Selected geometrical parameters are collected in Table 2, and the optimized equilibrium geometries of the *syn* isomers of **1a–1d** are displayed in Fig. 1(b). At the HF/6-31G(d) level, we find that the twisted *syn* isomers of **1a**, **1b**, and **1c** are 16.88, 17.05, and 18.02 kJ mol<sup>-1</sup> lower in energy than the twisted *anti* isomers, and the N=C—C=O and phenyl—C=O twist angles are

**Fig. 3.** The He(I) PE spectra of (a) **1a**, (b) the pyrolysate of **1a** obtained at a laser power level of 26 W, and (c) the pyrolysate of **1a** obtained at a laser power level of 42 W. The HAM/3//AM1 (vertical solid lines) and HAM/3//HF/6-31G(d) (vertical broken lines) calculated IPs are given in (a) for **1a** and (b) for **2a**.



approximately one-half the values calculated with AM1 (Table 2). This is most likely a result of the fact that the ab initio calculations more accurately recover the stabilizing phenyl—C=O— $\pi$  interaction, which would act to decrease the twist angle. When the geometries of the *syn* and *anti* isomers of **1a** were reoptimized — the geometries obtained with the default convergence limits were used as input — at the HF/6-31G(d) level of theory with the keyword TIGHT to tighten the convergence criteria, the total energies ( $E_T$ s) obtained were identical within  $10^{-6}$  hartree to  $E_T$ s calculated with the default convergence limits, and the geometries differed little from the input geometries (Table 2). These results are in accord with published experimental data: 1,4-bisdiazo-2,3-butanedione adopts a bis-*syn* conformation in the solid state (32), and variable-temperature solution <sup>1</sup>H NMR studies in the temperature range of +30 to -40°C showed that diazoketones of the type RCOCHN<sub>2</sub> (R=H, CH<sub>3</sub>, C<sub>2</sub>H<sub>5</sub>, *t*-C<sub>4</sub>H<sub>9</sub>, C<sub>6</sub>H<sub>5</sub>CH<sub>2</sub>, CH<sub>3</sub>O, and C<sub>2</sub>H<sub>5</sub>O) adopt *syn* and *anti* conformations with the *syn* forms being preferred (33). In the case of **1a**, **1c**, and **1e**, single stereoisomers identified as the *syn* forms were detected down to -40°C, but

**Fig. 4.** The He(I) PE spectra of (a) **1b**, (b) the pyrolysate of **1b** obtained at a laser power level of 26 W, and (c) the pyrolysate of **1b** obtained at a laser power level of 47 W. The HAM/3//AM1 (vertical solid lines) and HAM/3//HF/6-31G(d) (vertical broken lines) calculated IPs are given in (a) for **1b** and (b) for **2b**.

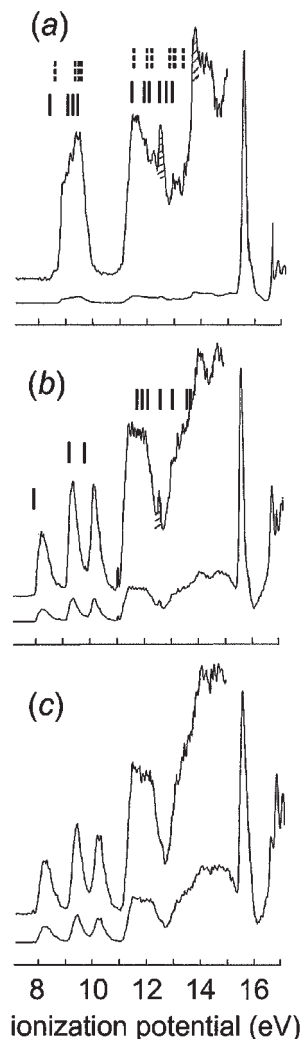
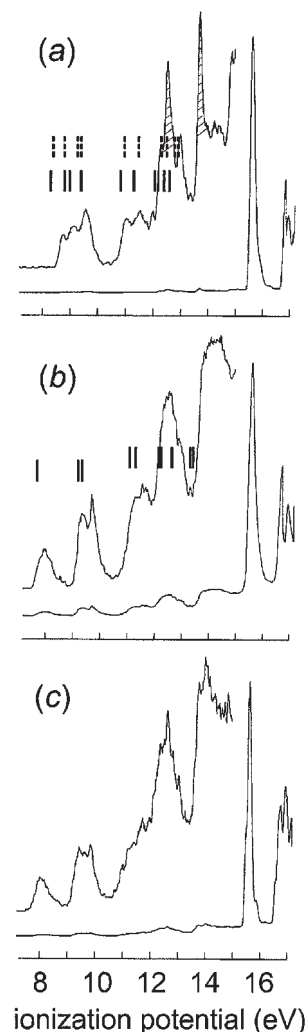


**Fig. 5.** The He(I) PE spectra of (a) **1c**, (b) the pyrolysate of **1c** obtained at a laser power level of 26 W, and (c) the pyrolysate of **1c** obtained at a laser power level of 42 W. The HAM/3//AM1 (vertical solid lines) and HAM/3//HF/6-31G(d) (vertical broken lines) calculated IPs are given in (a) for **1c** and (b) for **2c**.



N=C—C=O and phenyl—C=O twist angles were not determined (33).

Phenylketenes **2a–2e** are found to adopt planar conformations with AM1, in accordance with previous findings for **2a** (13). This also holds at the ab initio level, **2a–2e** are planar with HF/6-31G(d). The AM1 heats of formation and ab initio total energies of **2a–2e** are listed in Table 1. According to AM1, the 90° conformation of **2a** is destabilized by 9.04 kJ mol<sup>-1</sup>.

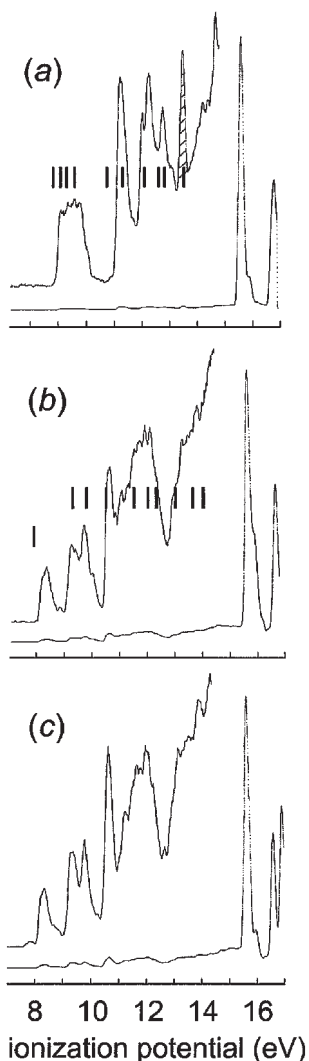
## 2. Ionization potentials

We have repeatedly demonstrated that the use of calculated ionization potentials (IPs) instead of orbital energies for the interpretation of PE spectra leads to excellent correlations between theory and experiment (2–4, 6, 34). This is

especially important where a good agreement between absolute energy values is needed, as is the case for highly reactive or transient species which are generated in the PE spectrometer itself. The semiempirical HAM/3 method gives IPs directly, and both semiempirical and ab initio optimized geometries can be employed. The HAM/3//AM1 and HAM/3//HF/6-31G(d) results for diazoacetophenones **1a–1c** are given in Table 3. Although AM1 and HF/6-31G(d) geometries for **1a–1c** are distinctly different, IP values from the two levels of theory differ little. We therefore report HAM/3//AM1 results only for phenylketenes **2a–2c**. Because HAM/3 is not parameterized for chlorine, we also use the routine we developed in previous publications (6, 34): orbital energies calculated with the hybrid HF/DFT Becke3LYP method<sup>3</sup> are shifted uniformly so that the

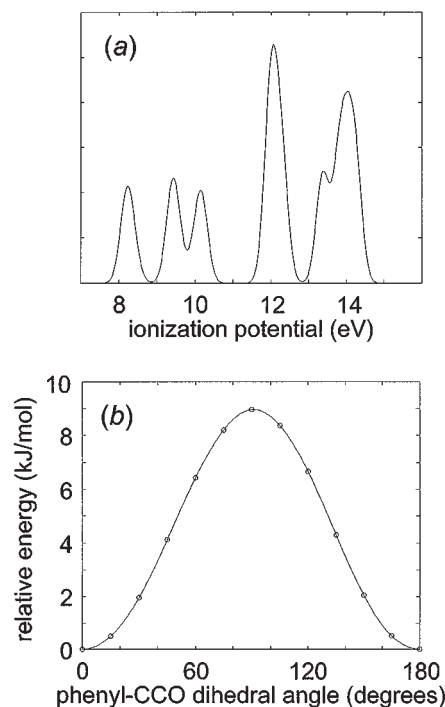
<sup>3</sup>The successful application of the Koopmans' theory-like (35) interpretation of orbital energies obtained at the DFT level of theory in PE spectroscopic studies of numerous compounds has been shown and commented on (6, 34, 36–38).

**Fig. 6.** The He(I) PE spectra of (a) **1d**, (b) the pyrolysate of **1d** obtained at a laser power level of 26 W, and (c) the pyrolysate of **1d** obtained at a laser power level of 42 W. The Becke3LYP/6-31+G(d)//HF/6-31G(d) (vertical solid lines) calculated IPs are given in (a) for **1d** and (b) for **2d**.



HOMO energy equals that of the calculated first vertical ionization potential  $IP_v$ . The  $IP_v$  is determined from the energy difference between the neutral (N electrons) and its radical cation (N - 1 electrons, geometry of the neutral) obtained using Becke3LYP/6-31+G(d)//HF/6-31G(d) (Table 4). Orbital energies and ionization potentials derived from the shift are reported in Table 3 for **1a–1d** and **2a–2d**. This level of theory is sufficient as could be concluded from virtually identical  $IP_v$ s and orbital energies of **2a–2d** obtained with Becke3LYP/6-31+G(d)//Becke3LYP/6-31+G(d) (not given).

**Fig. 7.** (a) Synthetic partial PE spectrum (from HAM/3//AM1 IPs) and (b) torsional potential (AM1) of **2a**.



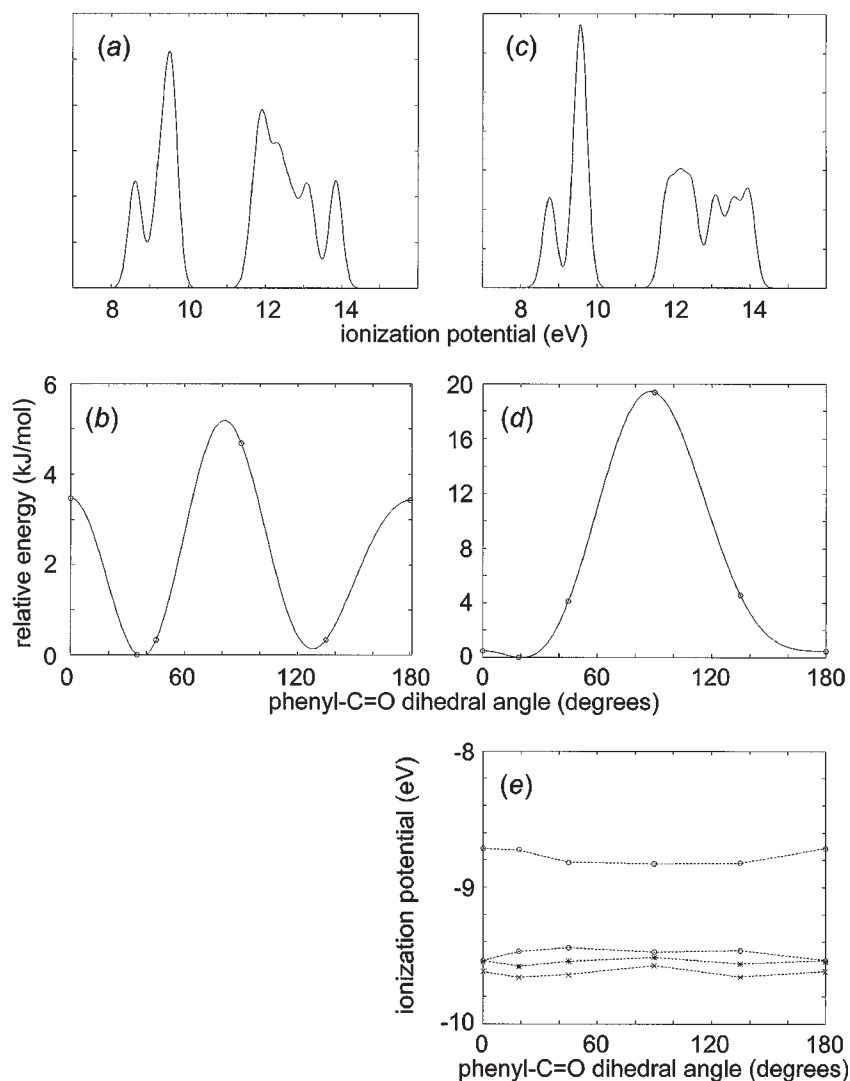
## Photoelectron spectroscopic studies

### 1. Experimental PE spectra

The spectrum of **1a** (20 mg; source pressure  $2.2 \times 10^{-3}$  Torr) displayed as Fig. 3(a) was obtained at a probe temperature of 50°C. The vertical solid lines and vertical broken lines on the spectrum correspond to the 10 lowest HAM/3//AM1 and HAM/3//HF/6-31G(d) IPs (values in Table 3), respectively, and show that the experimental spectrum of this diazoacetophenone can be reproduced nicely with HAM/3. Figure 3(b) is a display of the spectrum of the pyrolysate of **1a** obtained at a laser power of 26 W ( $\sim 500 \pm 50^\circ\text{C}$ ). Based on the 1:1:1 relative intensities of the bands at 8.2, 9.3, and 10.4 eV and excellent correlation between the experimental vertical IPs and the IPs of phenylketene (**2a**) calculated with HAM/3//AM1 (vertical solid lines), the conversion of **1a** to **2a** is complete at a laser power level of 26 W. The IPs for **1a** and **2a** calculated with Becke3LYP/6-31+G(d)//HF/6-31G(d) (Table 3, compare to experimental IPs in Table 5) give an equally good representation of both spectra and therefore support this. That there was no significant change in the spectrum of the pyrolysate (Fig. 3(c)) and no CO (it exhibits a sharp band at 14.01 eV (39)) was formed when the laser power was increased from 26 W to 42 W ( $\sim 850 \pm 50^\circ\text{C}$ ) indicates that the loss of CO from **2a** is subject to a high activation energy.<sup>4</sup> This observation is in keeping with the results of our previous calculational study (5). The spectrum of **2a** obtained in this study differs to

<sup>4</sup>A comprehensive computational study of the decomposition of **1a**, **1c**, and **1e** (loss of nitrogen) and **2a**, **2c**, and **2e** (loss of CO) as well as the rearrangement of the ketocarbenes derived from **1a**, **1c**, **1d**, and **1e** will be the subject of a following publication. As shown in Scheme 1, the pyrolyses of the diazoacetophenones are expected to proceed via the respective intermediate ketocarbenes, even though thermolysis spectra provide no evidence for this. Alternatively, extrusion of nitrogen and rearrangement could be a concerted process.

**Fig. 8.** (a) Synthetic partial PE spectrum (HAM/3//AM1), (b) surface for the torsion of the phenyl—C=O dihedral angle (AM1), (c) synthetic spectrum (HAM/3//HF/6-31G(d)), (d) torsional potential (HF/6-31G(d)), and (e) angular dependences of the four lowest HAM/3//HF/6-31G(d) IPs of **1a**.



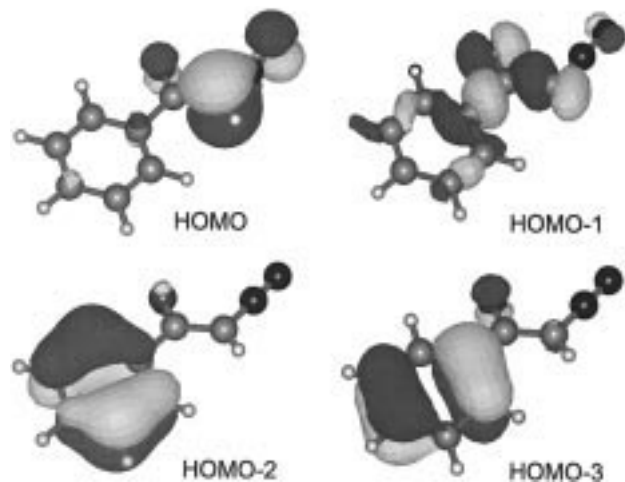
some degree from the published spectrum of phenylketene that was prepared by the zinc-induced dechlorination of 2-chloro-2-phenylacetyl chloride (**13**). While we find the relative areas of the first three bands to be 1:1:1 (Fig. 3(b)) in line with HAM/3//AM1 and Becke3LYP/6-31+G(d)//HF/6-31G(d) (Table 3) results, the relative areas of the first three bands of the previously published spectrum are approximately 1:2:1, an indication that phenylketene was not the sole product of the dechlorination reaction.

The spectrum of **1b** (20 mg; probe temperature 65°C), obtained with nitrogen added as a make-up gas to maintain the total pressure in the source at  $3 \times 10^{-3}$  Torr, is displayed along with the HAM/3//AM1 and HAM/3//HF/6-31G(d) IPs as Fig. 4(a). Again, HAM/3 values mirror experimental IPs. Figure 4(b) is a display of the spectrum of the pyrolysate of **1b** obtained at a laser power of 26 W and the calculated IPs of ketene **2b**. As in the case of the unsubstituted ketene **2a**, the experimental IPs in this spectrum are accurately reproduced by the computed values for **2b**, which shows that **1b**

cleanly yields *p*-methylphenylketene (**2b**). The IPs for **1b** and **2b** calculated using Becke3LYP (Table 3) agree with this finding. Figure 4(c) displays the PE spectrum of the pyrolysate of **1b** obtained at a laser power of 47 W (>900°C). That spectra in Figs. 4(b) and 4(c) are virtually identical and no CO is formed indicates that the activation energy for decarbonylating ketene **2b**, as in the case of **2a**, is significantly higher than the activation energy for loss of nitrogen from the respective diazoacetophenones.

Figure 5(a) displays the PE spectrum of **1c** obtained at a probe temperature of 76°C along with its HAM/3//AM1 and HAM/3//HF/6-31G(d) IPs. As in the case of **1b**, N<sub>2</sub> was used as a make-up gas to maintain the source pressure at  $3 \times 10^{-3}$  Torr. HAM/3 once more correctly predicts the experimental spectrum. The spectra displayed as Figs. 5(b) and (c) were obtained when **1c** was pyrolyzed at laser power levels of 26 and 42 W, respectively. These spectra show that **1c** cleanly affords *p*-methoxyphenylketene (**2c**), which does not undergo pyrolysis at a nozzle-tip temperature in the region

**Fig. 9.** The four highest occupied molecular orbitals of **1a**.



of  $850 \pm 50^\circ\text{C}$ . Again, HAM/3 and Becke3LYP IPs for **1c** and **2c** do not differ much, which shows the validity of our Becke3LYP approach.

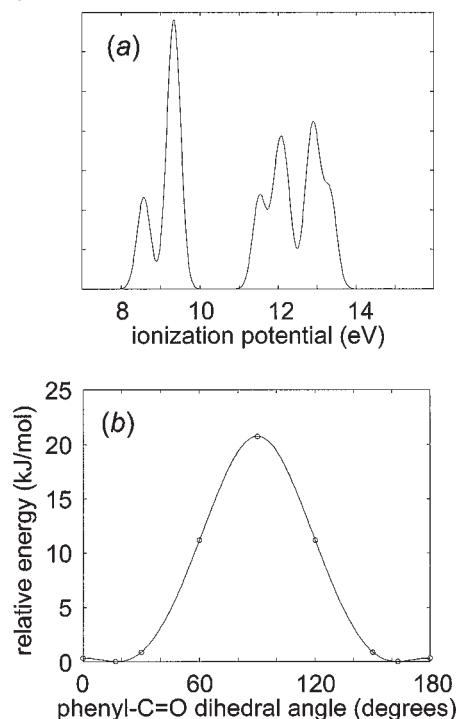
Figure 6(a) displays the PE spectrum of **1d** obtained at a probe temperature of  $55^\circ\text{C}$  with  $\text{N}_2$  added as a make-up gas to maintain the source pressure at  $3 \times 10^{-3}$  Torr. Figures 6(b) and (c) display spectra of the pyrolysate of **1d** obtained at laser power levels of 26 and 42 W, respectively. As HAM/3 is not parameterized for chlorine, Figs. 6(a) and (b) include the 10 lowest ionization potentials of **1d** and **2d** as calculated with Becke3LYP/6-31+G(d)//HF/6-31G(d) and described above. As expected from the encouraging results of the pyrolyses of **1a–1c** with respect to this approach, the correlation between predicted spectra (vertical bars) and experimental spectra is excellent. These spectra show that **1d** yields *p*-chlorophenylketene (**2d**), which also appears to be stable at a nozzle-tip temperature in the region of  $850 \pm 50^\circ\text{C}$ . The spectrum in Fig. 6(c) also exhibits a feature at 7.8 eV. A calculational study on *p*-chlorophenyloxirene, which is a second rearrangement product from the ketocarbene derived from **1d**, at the Becke3LYP/6-31+G(d)//HF/6-31G(d) level of theory established that the five lowest IPs of this compound should be 7.5, 9.6, 9.9, 11.0, and 11.7 eV. While the calculated first IP for *p*-chlorophenyloxirene is close to the first IP in the pyrolysis spectrum, at this point we cannot say with certainty whether it actually is a pyrolysis product of **1d**.<sup>5</sup>

The low volatility of **1e** thwarted our attempts to obtain its spectrum and study its pyrolysis. Even heating a relatively large sample (40 mg) of **1e** at  $94^\circ\text{C}$  near its melting point of  $116^\circ\text{C}$  in a 4 mm outer diameter tube inserted into the probe did not yield an acceptable spectrum. Selected experimental vertical ionization potentials of the diazoacetophenones **1a–1d** and the corresponding ketenes are collected in Table 5.

## 2. Synthesis of PE spectra

We have already demonstrated in several previous studies that PE spectra synthesized from torsional potential energy

**Fig. 10.** (a) Synthetic partial PE spectrum (HAM/3//HF/6-31G(d)) and (b) surface for the torsion of the phenyl–C=O dihedral angle (HF/6-31G(d)) of **1b**.

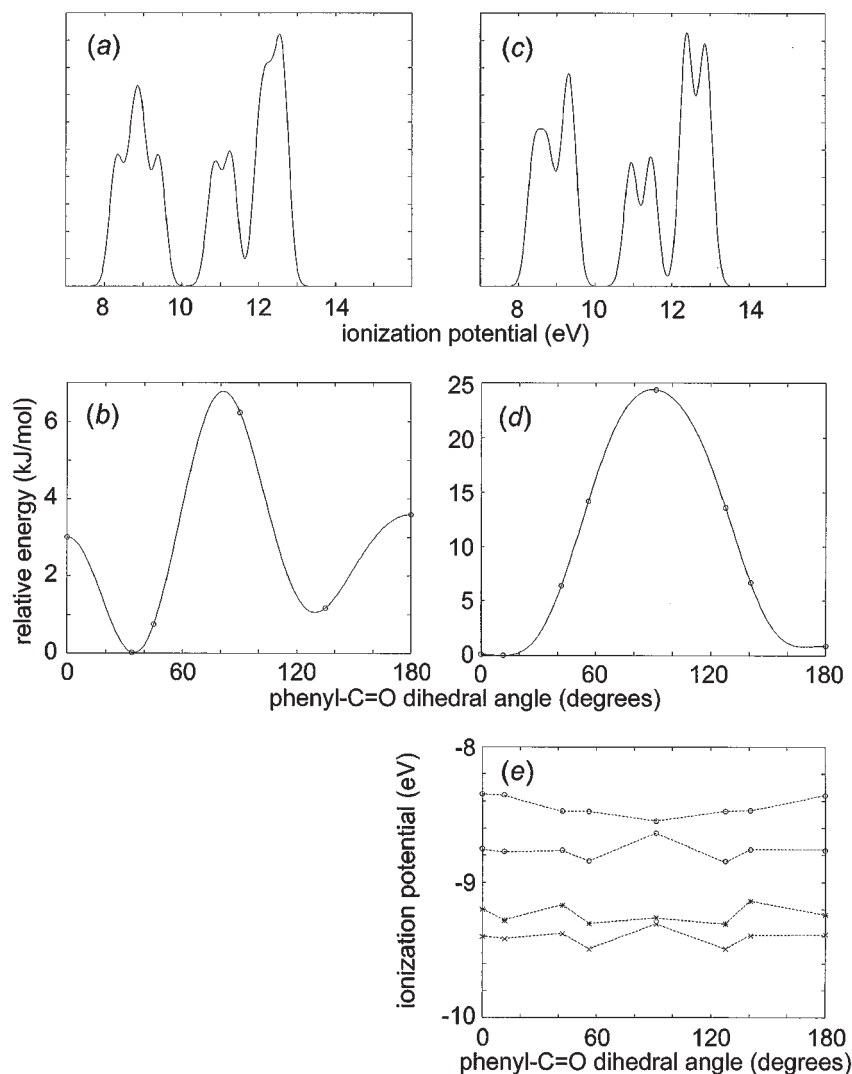


surfaces and the angle dependence of ab initio or semiempirical orbital energies as well as IPs calculated with HAM/3 using PESPEC correlate well with experimental spectra and can be used to obtain information about the conformational properties of molecules in the gas phase (29, 40–42). Additional support for this finding is seen in the excellent correlation between the experimental spectrum of phenylketene (**2a**) given in Figs. 3(b) and (c) and the synthesized spectrum displayed as Fig. 7(a). The synthetic spectrum of **2a** (with a Gaussian convolution of 0.4, temperature is 300 K) was obtained from the AM1 potential energy surface for the rotation of the ketene group given in Fig. 7(b) and the angle dependence of the 10 lowest HAM/3//AM1 ionization potentials (not shown).

While Modelli et al. (31) do not offer an interpretation of the spectra of **1a**, **1b**, and **1d** with respect to orbital interactions or conformational considerations, for **1a** Vorob'ev et al. (43) report only weak  $\pi$ - $\pi$  interactions both in the heterobutadiene group due to a large energy gap between interacting MOs and between diazo group and phenyl ring because of inefficient spatial overlap. Figure 8(a) is the PE spectrum of diazoacetophenone (**1a**) synthesized from the angle dependence of the HAM/3//AM1 IPs (not shown) and the AM1 potential energy surface displayed as Fig. 8(b) that corresponds to the 0– $180^\circ$  trajectory (the N=C–C=O dihedral angle is fixed at  $0^\circ$ ) of Fig. 2. The synthetic spectrum recovers the general features of the experimental spectrum. Figure 8(c) is the synthetic spectrum of **1a** obtained from the

<sup>5</sup>While from the first IP *p*-chlorophenyloxirene is a likely candidate, it will only be present in the pyrolysis gas mixture if there is a reasonable barrier to the reverse reaction, the ring opening of the three-membered ring to give the ketocarbene. Calculations for the rearrangement of ketocarbenes derived from diazoacetophenones **1a**, **1c**, and **1e** to the corresponding oxirenes have shown no significant barrier.<sup>4</sup>

**Fig. 11.** (a) Synthetic partial PE spectrum (HAM/3//AM1), (b) surface for the torsion of the phenyl—C=O dihedral angle (AM1), (c) synthetic spectrum (HAM/3//HF/6-31G(d)), (d) torsional potential (HF/6-31G(d)), and (e) angular dependences of the four lowest HAM/3//HF/6-31G(d) IPs of **1c**.



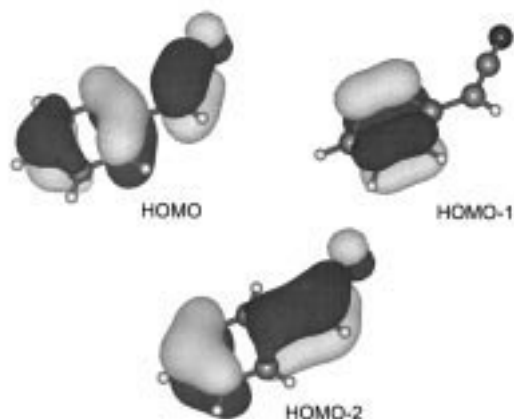
HF/6-31G(d) torsional potential (Fig. 8(d)) and the angular dependence of 10 HAM/3//HF/6-31G(d) IPs of which four are displayed in Fig. 8(e). Even though the rotational barrier at this level of theory is substantially higher than the AM1 barrier and the twisted *syn* conformer is only marginally lower in energy than the planar structure, the synthetic spectrum closely resembles the one obtained from the AM1 potential energy surface. This result derives from the fact that the low-energy IPs show a low sensitivity to the twist angle in both cases, as can be seen in Fig. 8(e). An explanation for this is given by the corresponding molecular orbitals (Fig. 9), which show that phenyl and diazoketo groups are present as separate units that do not interact at this energy level, a fact that was hinted at by Vorob'ev et al. (43).

According to Becke3LYP/6-31+G(d)//HF/6-31G(d),<sup>6</sup> the HOMO is a  $\pi$ -type orbital with coefficients mainly on the diazo group ( $\pi_{C=N}$ ), HOMO - 1 is a  $\sigma$ -type orbital, which represents an oxygen lone pair ( $n_O$ ), and HOMO - 2 and HOMO - 3 are mostly phenyl  $\pi$ -type MOs ( $\pi$ ) with small coefficients on the oxygen atom. This orbital sequence is in accord with the one given by Modelli et al. (31), while Vorob'ev et al. (43) give  $\pi_{C=N} > \pi > n_O > \pi$  from MNDO calculations. Thus in **1a**, which can be considered to be the parent of this class of compounds, the low lying occupied MOs of the carbonyl group effectively function as an insulator for phenyl and diazo moieties.

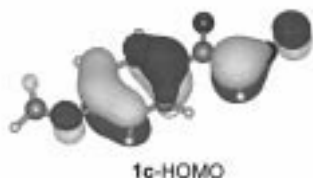
Figure 10(a) displays the synthetic spectrum of **1b** obtained from the torsional potential obtained at the HF/6-

<sup>6</sup>Even though there is "no physical relevance" to Kohn-Sham orbitals, we have found eigenvectors obtained at the Becke3LYP/6-31+G(d)//HF/6-31G(d) level of theory to be similar to those computed with HF/6-31G(d)//HF/6-31G(d) or AM1//HF/6-31G(d). Yet for a number of diazoketones and diazo acyl esters containing an aromatic ring the predicted orbital sequence differs at the above-mentioned levels of theory. In a following paper (44) we will show that in these cases the orbital sequence as determined with the Becke3LYP method should be taken. For this reason, the orbitals displayed in Fig. 9 are arranged according to the Becke3LYP/6-31+G(d)//HF/6-31G(d) calculated sequence.

**Fig. 12.** The three highest occupied molecular orbitals of **2a**.



31G(d) level (Fig. 10(b)) and the HAM/3//HF/6-31G(d) IPs (not shown). The torsional dependence of the IPs as well as the corresponding molecular orbitals are similar to what we found for **1a**. On the whole, the general features of the experimental spectrum are reproduced in the synthetic spectrum with reasonable accuracy even though there is baseline separation of one band from three overlapping bands. Figure 11(a) is the synthetic spectrum of **1c** obtained from the AM1 potential energy surface shown as Fig. 11(b). While the general features of band structure correlate with the PE spectrum, the relative intensities of the peaks of the low-IP band are at variance with the experimental data. On the other hand, the synthetic spectrum of **1c** (Fig. 11(c)) obtained from the HF/6-31G(d) torsional potential (Fig. 11(d)) and the angular dependence of 10 HAM/3//HF/6-31G(d) ionization potentials of which four are displayed in Fig. 11(e) closely resembles the experimental spectrum. In contrast to **1a** and **1b**, the HOMO of **1c** is a phenyl  $\pi$ -type orbital that is raised in energy above the  $\pi_{C=N}$  because of a substantial coefficient on the methoxy oxygen atom. This antibonding combination ( $\pi^-$ ) is followed by  $\pi_{C=N}$ ,  $n_O$ ,  $\pi$ , and the corresponding bonding combination ( $\pi^+$ ). As a consequence of this change in orbital sequence a phenyl  $\pi$ -type orbital ( $\pi^-$ ) and the  $\pi_{C=N}$  are closer in energy in **1c** than the respective orbitals in **1a**, which results in electron density on the diazo group being mixed into the HOMO of **1c**. Despite the presence of electron density on diazo group and aromatic ring, it is clear from Fig. 11(e) that the rotation of the ring does not affect the HOMO energy significantly, which again shows the insulating effect of the low-lying carbonyl orbitals. Our study shows that when compared to spectra synthesized on the basis of torsional potentials obtained at the HF/6-31G(d) level, experimental PE spectra provide



support that diazoacetophenones **1a–1d** prefer twisted *syn* conformations in the gas phase.

### Substituent effects on ionization potentials of phenylketenes

Figure 12 displays the HOMO, HOMO – 1, and HOMO – 2 of phenylketene (**2a**) obtained at the AM1//HF/6-31G(d) level. The HOMO is a  $\pi$ -type MO characterized by substantial antibonding mixing of the ketene and phenyl  $\pi$  systems, with the latter exhibiting a large  $p_z$  coefficient at C-4. The HOMO – 1 is a pure phenyl  $\pi$ -type MO, which does not mix with the ketene  $\pi$  system and which has no  $p_z$  component at C-4. The HOMO – 2 is the bonding  $\pi$ -type MO that, like the HOMO, has contributions from the ketene and phenyl groups. Nevertheless, it has a larger  $p_z$  coefficient at C-4 than the HOMO. The nature of these frontier MOs indicates that the HOMO and HOMO – 2 should be affected more strongly than HOMO – 1 by *para*-substituents, which interact with the phenyl ring via  $\pi$  conjugation. That this is the case is seen in the PE spectra of **2a** (Figs. 3(b) and (c)), **2b** (Figs. 4(b) and (c)), and **2c** (Figs. 5(b) and (c)), and the data in Table 5, which clearly show that HOMO and HOMO – 2 are destabilized by the introduction of  $\pi$  donors at C-4. That HOMO – 2 appears to be more sensitive to substitution at C-4 is a consequence of the size of the  $p_z$  component at C-4 and its proximity in energy to the other filled orbitals of lower energy with which it interacts.

### Conclusions

The gas-phase thermolysis of diazoacetophenones **1a–1d** at a laser power level of 26 W ( $500 \pm 50^\circ\text{C}$ ) gave the corresponding phenylketenes **2a–2d**, which do not decompose at higher laser power levels. A comparison of our PE spectrum of **2a** with the one published earlier indicates that the sample prepared in the previous study was impure. The low volatility of **1e** made the recording of its PE spectrum and the generation of **2e** impossible. According to AM1 and HF/6-31G(d) calculations, diazoacetophenones prefer twisted *syn* conformations in the gas phase. This is supported by excellent correlations between calculated ionization potentials of **1a–1d** at the HAM/3 and Becke3LYP/6-31+G(d)//HF/6-31G(d) levels of theory as well as simulated PE spectra of **1a–1c** and experimental spectra.

### Acknowledgments

We gratefully acknowledge the usage of the IBM SP2 computer at Queen's University granted under the auspices of an IBM Canada – Queen's University collaborative project as well as the usage of the SGI computing installation in the Geochemistry Labs at McMaster funded by NSERC. We thank Ms. O. Donini for assistance with operational aspects of parallel GAUSSIAN 94 and the Natural Sciences and Engineering Research Council of Canada for financial support.

### References

1. N.H. Werstiuk, C.D. Roy, and J. Ma. *Can. J. Chem.* **72**, 2537 (1994).
2. N.H. Werstiuk, C.D. Roy, and J. Ma. *Can. J. Chem.* **73**, 146 (1995).

3. N.H. Werstiuk, J. Ma, C.D. Roy, A.J. Kresge, and E.A. Jefferson. *Can. J. Chem.* **73**, 1738 (1995).
4. N.H. Werstiuk, C.D. Roy, and J. Ma. *Can. J. Chem.* **74**, 1903 (1996).
5. N.H. Werstiuk, J. Ma, C.D. Roy, A.J. Kresge, and E. Jefferson. *Can. J. Chem.* **74**, 2536 (1996).
6. H.M. Muchall, N.H. Werstiuk, B. Choudhury, J. Ma, J. Warkentin, and J.P. Pezacki. *Can. J. Chem.* **76**, 238 (1998).
7. L. Wolff. *Justus Liebigs Ann. Chem.* **394**, 23 (1912).
8. D. Colbourne, D.C. Frost, C.A. McDowell, and N.P.C. Westwood. *J. Chem Soc. Chem. Commun.* 250 (1980).
9. A. Hotzel, R. Neidlein, R. Schultz, and A. Schweig. *Angew. Chem. Int. Ed. Engl.* **19**, 739 (1980).
10. S. Mohmand, T. Hirabayashi, and H. Bock. *Chem. Ber.* **114**, 2595 (1981).
11. D.P. Chong, N.P.C. Westwood, and S.R. Langhoff. *J. Phys. Chem.* **88**, 1479 (1984).
12. D. Colbourne and N.P.C. Westwood. *J. Chem. Soc. Perkin Trans. II*, 2049 (1985).
13. R. Sammynaiken and N.P.C. Westwood. *J. Chem. Soc. Perkin Trans. II*, 1987 (1989).
14. The chemistry of the diazonium and diazo groups. Parts 1 and 2. *Edited by S. Patai*. John Wiley and Sons, New York. 1978.
15. W. Kirmse. *In Advances in carbene chemistry*. Vol. 1. *Edited by U.H. Brinker*. JAI Press Inc., Greenwich, Conn. 1994.
16. B.M. Trost and P.L. Kinson. *J. Am. Chem. Soc.* **97**, 2438 (1975).
17. R.J. McMahon, O.L. Chapman, R.A. Hayes, T.C. Hess, and H.-P. Krimmer. *J. Am. Chem. Soc.* **107**, 597 (1985).
18. A. Allen, A.J. Kresge, N.P. Schepp, and T.T. Tidwell. *Can. J. Chem.* **65**, 1719 (1987).
19. R.J. McMahon, C.J. Abelt, O.L. Chapman, J.W. Johnson, C.L. Kreil, J.-P. LeRoux, A.M. Mooring, and P.R. West. *J. Am. Chem. Soc.* **109**, 2456 (1987).
20. C. Bachman, T.Y. N'Guessan, F. Debû, M. Monnier, J. Pourcin, J.-P. Aycard, and H. Bodot. *J. Am. Chem. Soc.* **112**, 7488 (1990).
21. J. Andraos and A.J. Kresge. *J. Photochem. Photobiol. A*, **57**, 165 (1991).
22. HYPERCHEM 4.0. Hypercube Inc., 419 Philip Street, Waterloo, Ont. 1994.
23. Dewar Research Group and J.J.P. Stewart. Austin Model 1 Package 1.0 (AMPAC). QCPE, 506 (1986).
24. J.J.P. Stewart. MOPAC, a semiempirical molecular orbital program. QCPE, 455 (1983).
25. W.J. Hehre, L. Radom, P.v.R. Schleyer, and J.A. Pople. *Ab initio molecular orbital theory*. John Wiley & Sons, New York. 1986.
26. A.D. Becke. *J. Chem. Phys.* **98**, 5648 (1993); C. Lee, W. Yang, and R.G. Parr. *Phys. Rev. B: Condens. Matter*, **37**, 785 (1988).
27. M.J. Frisch, G.W. Trucks, H.B. Schlegel, P.M.W. Gill, B.G. Johnson, M.A. Robb, J.R. Cheeseman, T. Keith, G.A. Petersson, J.A. Montgomery, K. Raghavachari, M.A. Al-Laham, V.G. Zakrzewski, J.V. Ortiz, J.B. Foresman, C.Y. Peng, P.Y. Ayala, W. Chen, M.W. Wong, J.L. Andres, E.S. Replogle, R. Gomperts, R.L. Martin, D.J. Fox, J.S. Binkley, D.J. Defrees, J. Baker, J.P. Stewart, M. Head-Gordon, C. Gonzalez, and J.A. Pople. Gaussian 94, Revision B.3. Gaussian, Inc., Pittsburgh Pa. 1995.
28. L. Åsbrink, C. Fridh, and E. Lindholm. *HAM/3, QCPE Bull.* **13**, 393 (1981).
29. N.H. Werstiuk, G. Timmins, G. Ma, and T.A. Wildman. *Can. J. Chem.* **70**, 1971 (1992).
30. M. Regitz and F. Menz. *Chem. Ber.* **101**, 2622 (1968).
31. A. Modelli, G. Innorta, and S. Torrioni. *J. Electron Spectrosc. Relat. Phenom.* **18**, 359 (1980).
32. H. Hope and K.T. Black. *Acta Crystallogr. Sect. B: Struct. Crystallogr. Cryst. Chem.* **28**, 3632 (1972).
33. F. Kaplan and G.K. Meloy. *J. Am. Chem. Soc.* **88**, 950 (1966).
34. H.M. Muchall, N.H. Werstiuk, and B. Choudhury. *Can. J. Chem.* **76**, 221 (1998).
35. T. Koopmans. *Physica*, **1**, 104 (1933).
36. A.J. Arduengo, III, H. Bock, H. Chen, M. Denk, D.A. Dixon, J.C. Green, W.A. Herrmann, N.L. Jones, M. Wagner, and R. West. *J. Am. Chem. Soc.* **116**, 6641 (1994).
37. H.M. Muchall and P. Rademacher. *J. Mol. Struct.* **435**, 157 (1997).
38. N.H. Werstiuk, H.M. Muchall, C.D. Roy, J. Ma, and R.S. Brown. *Can. J. Chem.* **76**, 672 (1998).
39. K. Kimura, K. Katsumata, Y. Achiba, T. Yamazaki, and S. Iwata. *Handbook of HeI photoelectron spectra of fundamental organic molecules*. Japan Scientific Societies Press, Tokyo, and Halsted Press, New York. 1981.
40. N.H. Werstiuk, J. Ma, M.A. McAllister, T.T. Tidwell, and D.-C. Zhao. *Trans. Faraday Soc.* **90**, 3383 (1994).
41. D. Chmielewski, N.H. Werstiuk, and T.A. Wildman. *Can. J. Chem.* **71**, 1741 (1993).
42. H.M. Muchall, N.H. Werstiuk, J. Ma, T.T. Tidwell, and K. Sung. *Can. J. Chem.* **75**, 1851 (1997).
43. A.S. Vorob'ev, I.I. Furlei, Yu.Z. Ekov, A.M. Nazarov, G.A. Yamilova, U.M. Dzhemilev, and V.A. Dokichev. *Russ. Chem. Bull.* **42**, 281 (1993).
44. H.M. Muchall, N.H. Werstiuk, J.L. Pitters, and M.S. Workentin. *Tetrahedron*. In press.